CHEMISTRY
A EUROPEAN JOURNAL

FULL PAPER

DOI: 10.1002/chem.201301380

# Theoretical Modelling of Photoswitching of Hyperpolarisabilities in Ruthenium Complexes

**Benjamin J. Coe,*[a] Aggelos Avramopoulos,[b] Manthos G. Papadopoulos,[b] Kristine Pierloot,[c] Steven Vancoillie,[c] and Heribert Reis*[b]**

**Abstract:** Static excited-state polarisabilities and hyperpolarisabilities of three $Ru^{II}$ ammine complexes are computed at the density functional theory (DFT) and several correlated ab initio levels. Most accurate modelling of the low energy electronic absorption spectrum is obtained with the hybrid functionals B3LYP, B3P86 or M06 for the complex $[Ru^{II}(NH_3)_5(MeQ^+)]^{3+}$ ($MeQ^+ = N$-methyl-4,4′-bipyridinium, **3**) in acetonitrile. The match with experimental data is less good for $[Ru^{II}(NH_3)_5L]^{3+}$ (L = *N*-methylpyrazinium, **2**; *N*-methyl-4-{*E*,*E*-4-(4-pyridyl)buta-1,3-dienyl}pyridinium, **4**). These calculations confirm that the first dipole-allowed excited state (FDAES) has metal-to-ligand charge-transfer (MLCT) character. Both the solution and gas-phase results obtained for **3** by using B3LYP, B3P86 or M06 are very similar to those from restricted active-space SCF second-order perturbation theory (RASPT2) with a very large basis set and large active space. However, the time-dependent DFT $\lambda_{max}$ predictions from the long-range corrected functionals CAM-B3LYP, LC-ωPBE and wB97XB and also the fully ab initio resolution of identity approximate coupled-cluster method (gas-phase only) are less accurate for all three complexes. The ground state (GS) two-state approximation first hyperpolarisability $\beta_{2SA}$ for **3** from RASPT2 is very close to that derived experimentally via hyper-Rayleigh scattering, whereas the corresponding DFT-based values are considerably larger. The $\beta$ responses calculated by using B3LYP, B3P86 or M06 increase markedly as the π-conjugation extends on moving along the series **2**→**4**, for both the GS and FDAES species. All three functionals predict substantial FDAES $\beta$ enhancements for each complex, increasing with the π-conjugation, up to about sevenfold for **4**. Also, the computed second hyperpolarisabilities $\gamma$ generally increase in the FDAES, but the results vary between the different functionals.

**Keywords:** density functional caclulations · molecular switches · nonlinear optics · ruthenium complexes

## Introduction

The promise of diverse applications including optical data processing and biological imaging has stimulated much interest in organic nonlinear optical (NLO) materials.[1] Within this field, organotransition metal complexes offer intriguing possibilities for creating new multifunctional materials in which potentially useful optical behaviour is combined with the redox, magnetic and other properties characteristic of such compounds.[2] As a means to enhance the prospects for molecular materials, approaches to modulating reversibly molecular NLO properties have attracted considerable attention recently.[3] The first report of a very pronounced and reversible redox-switching of the first hyperpolarisability $\beta$ (the origin of quadratic molecular NLO effects) clearly demonstrated the potential significance of metal complexes in this area.[4] This work has been extended to second harmonic generation (SHG) in Langmuir–Blodgett (LB) thin films,[5] and various related solution and molecular-level theoretical studies involving both quadratic and cubic NLO effects have been described.[6]

Although the switching of NLO responses via redox chemistry has attracted much attention, using other stimuli is also of great interest. Light-induced (photochromic) molecular rearrangements have been explored relatively widely.[3,7] However, the speed of switching accompanying such structural changes is often quite limited, and their effects on macroscopic structures may be substantial. Populating transient electronic excited states should allow much faster modulation effects without significant structural changes. Early CNDO/S calculations on some simple dipolar molecules, such as 4-nitroaniline, indicated that $\beta$ responses

[a] Dr. B. J. Coe
School of Chemistry, University of Manchester
Oxford Road, Manchester M13 9PL (UK)
E-mail: b.coe@manchester.ac.uk

[b] Dr. A. Avramopoulos, Dr. M. G. Papadopoulos, Dr. H. Reis
Institute of Biology, Medicinal Chemistry and Biotechnology
National Hellenic Research Foundation
48 Vas. Constantinou Avenue, Athens 11635 (Greece)
E-mail: hreis@eie.gr

[c] Prof. Dr. K. Pierloot, Dr. S. Vancoillie
Department of Chemistry, University of Leuven
Celestijnenlaan 200F, Box 2404, 3001 Heverlee-Leuven (Belgium)

can be increased in excited states,[8] and these predictions were verified subsequently.[9] Various experimental studies with purely organic chromophores reveal similar behaviour, mostly focusing on second hyperpolarisabilities $\gamma$,[10] and attempts to determine excited-state $\beta$ values by hyper-Rayleigh scattering (HRS) have been reported.[11] However, such measurements are fraught with complications and hence there is currently no reliable experimental method by which such molecular-level excited-state responses can be determined. Therefore, the establishment of accurate theoretical approaches is of significant interest, as a guide to empirical studies that will most likely focus on the switching of bulk effects like SHG.

Some time ago, Sakaguchi et al. noted a small photoinduced switching of SHG at 295 nm from alternating and highly diluted LB films containing the amide-substituted $[Ru^{II}(2,2'\text{-bpy})_3]^{2+}$ (bpy = bipyridyl) derivative **1** (Figure 1).[12] This observation was attributed to changes in $\beta$ on MLCT excitation. However, the ground-state (GS) complex shows an intense 2,2′-bpy-based absorption near the SHG wavelength, so excitation-induced changes in absorption may affect the SHG signal. Notably, very few other related experimental or theoretical studies with metal complexes have been reported to our knowledge (and these concern only $\gamma$ responses).[13]

The $[Ru^{II}(NH_3)_5]^{2+}$ complexes that we have studied as redox-switchable NLO chromophores[4,5] show intense MLCT bands in the visible region. Consequently, they show very large $\beta$ responses that compare favourably with those

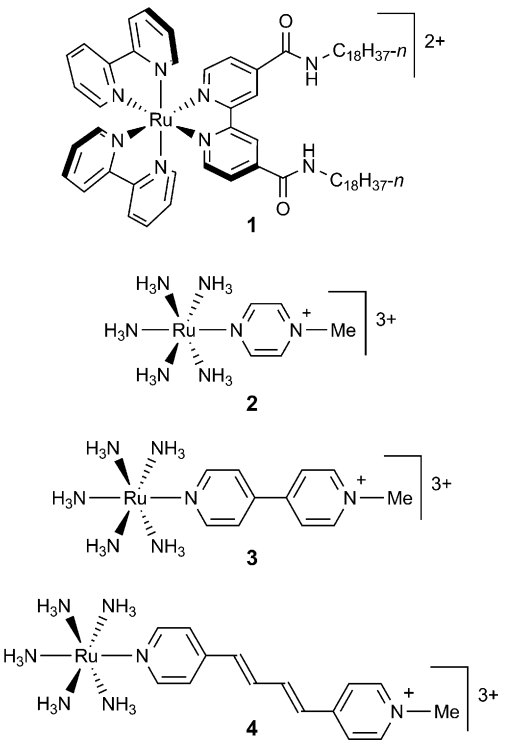


Figure 1. A ruthenium complex (**1**) studied previously for ps timescale photoswitching of SHG in LB films,[12] and the complexes **2**–**4** considered in the present work.

of purely organic chromophores with moderate π-conjugation lengths.[2i,14] These systems are therefore highly attractive subjects for photoswitching studies, and we describe here theoretical investigations, which indicate that MLCT excitations lead to large changes in molecular NLO responses. The use of time-dependent density functional theory (TD-DFT) and ab initio methods to predict hyperpolarisabilities of GS chromophores is now well developed,[15] but relevant considerations of electronic excited states are restricted to polarisabilities and/or small molecules.[16]

## Results and Discussion

Our calculations focus on the series of complexes **2**–**4** (Figure 1). Complex **2** is well studied,[17] and Stark spectroscopy in a 1:1 glycerol/water glass has been used to derive a modest static first hyperpolarisability $\beta_0$ ($<10^{-29}$ esu) for the salt $[\mathbf{2}][BF_4]_3$.[18] We have used HRS in acetonitrile (MeCN) solutions and Stark measurements in butyronitrile (PrCN) glasses to afford substantially larger $\beta_0$ values (HRS/Stark, $10^{-30}$ esu) of 246/240 for $[\mathbf{3}][PF_6]_3$[19,20] and 744/1092 for $[\mathbf{4}][PF_6]_3$.[21] Note that we consistently use the so-called *T*-convention in this work,[22] whereas previous reports[19–21] use the *B*-convention; to convert to the *T*-convention, we use $\beta_T = 2\beta_B$. In addition, all of our values refer to the dominant component along the long molecular axis, approximately parallel to the dipole moment. The pronounced increases in NLO response on moving along the series **2**→**4** are consistent with their steadily extending π-conjugated structures.

In order to determine the most appropriate theoretical method for treating Ru ammine complexes, we have tried various approaches to model the MLCT excited states. Previous gas-phase DFT calculations using the B3P86 functional with the LANL2DZ basis set proved qualitatively useful, but lack quantitative accuracy.[21] A similar basis set combination LANL2DZ(Ru)/6-31G* or 6-31+G*(H,C,N,O) has been used by Inerbaev et al.,[23] and in a recent investigation by Zhang and Champagne.[24] Here, we use a larger basis set (LANL2TZ(f)) for Ru in DFT calculations, as well as different larger basis sets for various high-level ab initio methods. We provide a more detailed account of the methodology in the Computational Methods.

Comparing the new computational results with the experimental data shows that TD-DFT with the hybrid functionals B3LYP, B3P86 or M06 yields very good values for the first dipole-allowed excited state (FDAES) of **3**, when MeCN solvent is included via the polarisable continuum model (PCM; Table 1). Selected simulated spectra are shown in Figure 2, together with the experimental spectra of complexes **3** and **4** as their $PF_6^-$ salts. Comparisons with data published previously[23,24] show that although using a larger basis set for Ru does not affect the qualitative picture of the excitation properties, some significant quantitative differences are observed.

The excitation into the FDAES consists for **3** and **4** nearly exclusively of the HOMO→LUMO transition, whereas for

  

Table 1. Selected data calculated for complexes **2**–**4** by using DFT and ab initio methods,[a] together with previously reported measured data.

| Method | 2 | | 3 | | 4 | |
|---|---|---|---|---|---|---|
| | $\lambda_{max}$ [nm] | $f_{os}$ | $\lambda_{max}$ [nm] | $f_{os}$ | $\lambda_{max}$ [nm] | $f_{os}$ |
| B3LYP | 439 | 0.28 | 449 | 0.24 | 439 | 0.86 |
| B3LYP/solvent[b] | 456 | 0.49 | 578 | 0.35 | 641 | 0.69 |
| | | | | | 408[c] | 1.32[c] |
| M06/solvent | 472 | 0.48 | 599 | 0.37 | 659 | 0.71 |
| B3P86 | 437 | 0.28 | 454 | 0.25 | 444 | 0.81 |
| B3P86/solvent | 455 | 0.50 | 587 | 0.36 | 654 | 0.70 |
| | | | | | 407[c] | 1.32[c] |
| M06L/solvent | 455 | 0.46 | 788 | 0.39 | 937 | 0.64 |
| CAM-B3LYP | 404 | 0.27 | 332 | 0.17 | 356 | 1.81 |
| CAM-B3LYP/solvent | 434 | 0.48 | 379 | 0.42 | 416 | 1.68 |
| wB97XD | 408 | 0.27 | 333 | 0.12 | 353 | 1.82 |
| LC-ωPBE | 374 | 0.25 | 277 | 0.42 | 329 | 1.20 |
| LC-ωPBE/solvent | 393 | 0.37 | 305 | 0.42 | 347 | 1.74 |
| RI-CC2/def2-TZVPP | 615 | 0.42 | 421 | 0.34 | 389 | 0.53 |
| | | | | | 389 | 0.57 |
| RASPT2(18,18)[d] | | | 437 | 0.22 | | |
| RASPT2(18,18)/MeCN[d] | | | 585 | 0.21 | | |
| B3P86/LANL2DZ[e] | | | 482 | 0.37 | 473 | 0.79 |
| | | | | | 366 | 1.06 |
| B3P86/LANL2DZ/MeCN[f] | | | 608 | | 693 | |
| B3P86/6-31G*/LANL2DZ(Ru)/ MeCN[g] | | | 546 | 0.29 | 607 | 0.57 |
| | | | | | 386 | 1.12 |
| measured[h] | 540 | | 590 | 0.20 | 584 | 0.43 |
| | | | | | 354 | 0.58 |

[a] Molecules **2** and **3** were optimised with B3LYP/6-31G**/LANL2TZ(f) (Ru), whereas 6-31G* was used for **4**. All optimisations were performed in the gas phase, except for **2**, which was optimised in the gas phase and in $H_2O$. [b] MeCN used as solvent for **3** and **4**, $H_2O$ used for **2**. [c] For the second dipole-allowed excited state (SDAES). [d] State-averaged RASPT2. [e] Data taken from ref. [21]. [f] Data taken from ref. [23]. [g] Data taken from ref. [24]. [h] For **[2]**$[ClO_4]_3$ in $H_2O$ (a very weak NIR band at $\lambda_{max}$ = 855 nm is observed also),[17c] **[3]**$[PF_6]_3$,[19] and **[4]**$[PF_6]_3$;[21] $\lambda_{max}$ values in MeCN at room temperature; directly corresponding $f_{os}$ values are unavailable, so those quoted are in PrCN at 77 K (only slight variations due to changing the solvent and temperature are expected).[20]

**2** it is a HOMO−1→LUMO transition. The orbitals, shown in Figure 3 for B3LYP as an example, demonstrate clearly that in each case a charge transfer from Ru to the organic ligand is involved, confirming the expected MLCT character. To better quantify these transitions, we have applied a model developed by Bahers et al. recently for the semi-quantitative analysis of photoinduced CT processes, which is based on the differences in electron density between the ground and excited states.[25] Figure 4 shows the spatially-resolved density differences upon excitation for the three complexes. This model also affords estimates of the transferred charge $q_{CT}$ and the CT distance $r_{CT}$, which are 0.288 e/1.571 Å for **2**, 0.953 e/4.218 Å for **3**, and 0.978 e/5.799 Å for **4**, evaluated for B3LYP. To put these data into perspective, we note that the corresponding values for the prototypical CT molecule 4-nitroaniline in MeCN are 0.62 e/2.72 Å.[25c] The calculated $r_{CT}$ values agree relatively well with the effective (localised) electron-transfer distances $r_{ab}$ calculated from $\Delta_{01}\mu_{ab}/e$, where $\Delta_{01}\mu_{ab}$ is the dipole-moment change between the diabatic states involved in the MLCT transition. Based on Stark spectroscopic measurements, respective $r_{ab}$ values of 3.6 and 5.7 Å are determined for **[3]**$[PF_6]_3$ and **[4]**$[PF_6]_3$ in PrCN glasses at 77 K.[20,21]

The predicted $\lambda_{max}$ values agree less well with those measured for **4**, and the observed blue shift in the MLCT band on moving from **3** to **4** is not reproduced in solution. However, this blue shift is predicted by the gas-phase results, albeit with a decrease in the overall accuracy of the $\lambda_{max}$ values, reminiscent of previous gas-phase B3P86/LanL2DZ calculations.[21] Our new calculations using B3LYP, B3P86 or M06 give rather large discrepancies between theory and experiment for **2**. Nonetheless, it is gratifying that the results obtained for **3** by using these functionals are very similar to those from high-level restricted active-space SCF second-order perturbation theory (RASPT2) with a very large basis set and large active space (see the Computational Methods for details), both in solution and the gas-phase. The long-range corrected functionals (LRCFs) CAM-B3LYP,[26] LC-ωPBE[27] and wB97XB[28] give $\lambda_{max}$ predictions less accurate than those obtained when using B3LYP, B3P86 or M06 for all three complexes (see also Figure 2b). These results are quite surprising because one of the reasons LRCFs were introduced was specifically to improve descriptions of charge-transfer excitations by standard DFT functionals.[26–28] However, our results concur with other recent studies on organotransition metal compounds.[29] For example, Escudero and González[29c] found poor performance by CAM-B3LYP and LC-ωPBE for MLCT excitations in *trans*-$[RuCl_2(2,2'\text{-bpy})(CO)_2]$, when compared to experimental and RASPT2 results, with more accurate predictions from hybrid functionals. The reasons for such unsatisfactory performance of LRCFs are unclear at present.

Although only gas-phase results are available for the fully ab initio and reasonably high-level resolution of identity approximate coupled-cluster (RI-CC2) method, they differ substantially from those derived from DFT and RASPT2, and notably overestimate $\lambda_{max}$ when compared with experiment for **2**. For **4**, RI-CC2 predicts two very close-lying transitions ($\lambda_{max}$ = 389 nm) of comparable intensity, which is also not predicted by any other method. The relative failure of RI-CC2 may derive from the rather large values of the $D_1$ diagnostic for the CC2 GS wavefunction (0.317, 0.124 and 0.115 for **2**, **3** and **4**, respectively). Values of $D_1$ above 0.050 may indicate a large multi-configurational character of the GS, for which the single-reference method CC2 is not suitable.[30] However, without taking into account the apparently large solvent effect, it is difficult to judge the performance of RI-CC2 with confidence. As a general point, we note that DFT takes into account the non-dynamical correlation, although only partially and in a non-systematic way.[31] This aspect may explain why the method performs better for complex **3** than for **2**, which according to the $D_1$ diagnostic

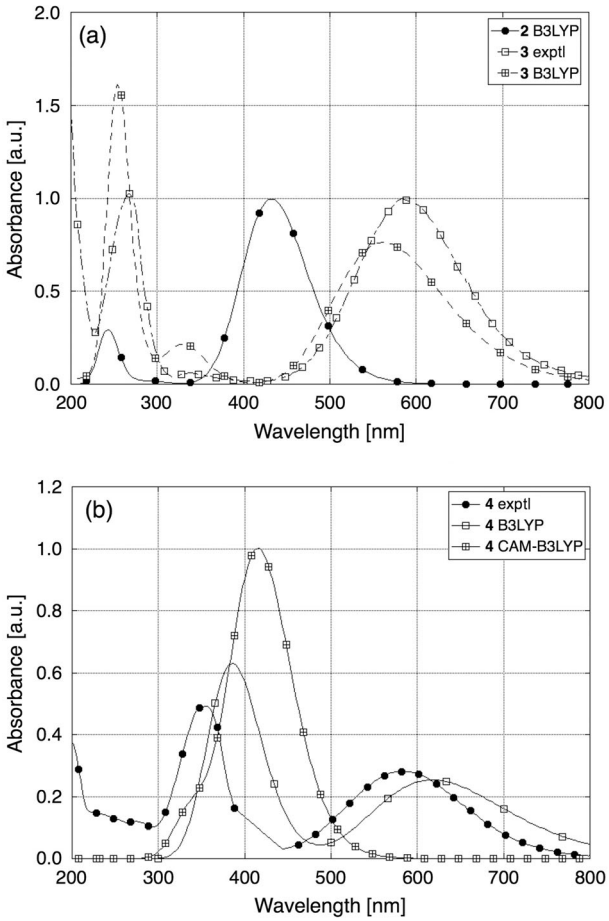


Figure 2. a) Normalised electronic absorption spectra of **2** (simulated) and **3** (simulated and experimental) in solution; all the simulated spectra are convolutions of the computed B3LYP values with a Gaussian function with $\sigma = 2000\ cm^{-1}$. b) Experimental and simulated electronic absorption spectra of **4**; both CAM-B3LYP and B3LYP simulated spectra are shown. The experimental data were obtained with the complex salts [**3**][$PF_6$]$_3$ or [**4**][$PF_6$]$_3$ in MeCN.[19,21]

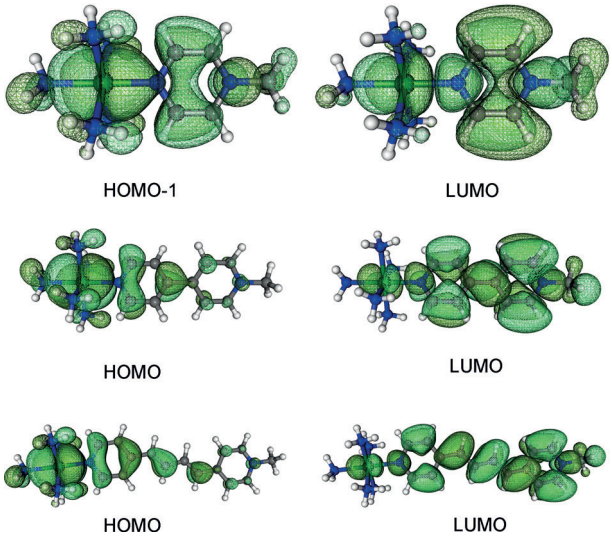


Figure 3. Orbitals (B3LYP) involved in the main transition from the GS to the FDAES for **2** (top), **3** (middle) and **4** (bottom).

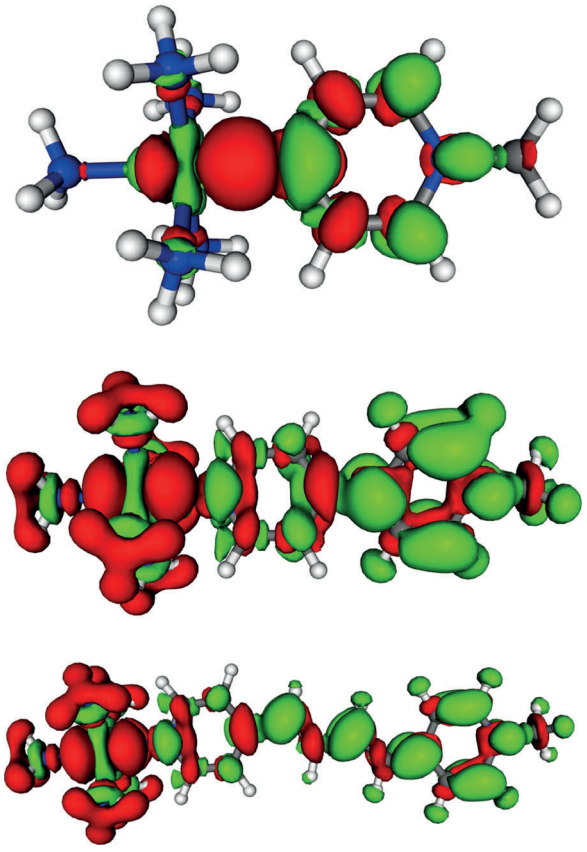

Figure 4. Plots showing difference electron density between the GS and the FDAES of **2** (top), **3** (middle) and **4** (bottom); green denotes positive differences, whereas negative differences are in red; isocontour values ±0.001.

from CC2 may have stronger multi-configurational character. This point is still under investigation.

Further tests using different optimised geometries show that the geometry does not have a large influence on $\lambda_{max}$ or $f_{os}$. This observation validates the comparisons between the results of the RASPT2 calculations for **3**, which for computational efficiency reasons used a geometry of $C_s$ symmetry, and the data obtained from the other methods that used a $C_1$ symmetry. The relative geometry independence holds also for the NLO properties of **3** and **4**, but not for those of **2**. Therefore, all of the properties of **2** were computed with the geometry optimised in the corresponding environment (gas-phase or water solvent).

Considering that the NLO properties are very dependent on a good description of the excited-state manifold, it seems that, apart from highly accurate (and computationally expensive) multi-configurational methods, only the properties calculated with B3LYP, B3P86 or M06 may be at least approximately reliable. Therefore, parameters for the GS and FDAES derived by using these functionals for the complexes embedded in a solvent continuum are collected in Table 2, together with CAM-B3LYP results. All of the (hyper)polarisabilities were computed by finite-field derivatives

  

Table 2. Further data calculated for complexes **2**–**4** by using DFT and RASPT2 methods,[a] together with previously reported measured data.

| Complex | Method | State | $\mu_z$ [au] | $\alpha_{zz}$ [au] | $\beta_{zzz}$ [$10^3$ au] | $\gamma_{zzzz}$ [$10^4$ au] | $\Delta_{01}\mu_z/\Delta_{02}\mu_z$ [au] | $\Delta_{01}\alpha_{zz}$ [au] | $\mu_{01}/\mu_{02}$ [au] | $\beta_{2SA}/\beta_{3SA}$[b] [$10^3$ au] |
|---|---|---|---|---|---|---|---|---|---|---|
| **2** | B3LYP | GS | 0.37 | 336 | 6 | −4 | | | 2.71 | 3.8 |
| | | FDAES | 1.23 | 224 | 17 | 22 | 0.86 | −112 | | |
| | B3P86 | GS | 0.42 | 337 | 6 | −5 | | | 2.74 | 3.7 |
| | | FDAES | 1.25 | 229 | 17 | 11 | 0.83 | −108 | | |
| | M06 | GS | 0.57 | 346 | 5 | −15 | | | 2.74 | 2.6 |
| | | FDAES | 1.11 | 246 | 17 | 3 | 0.54 | −100 | | |
| | CAM-B3LYP | GS | −0.16 | 310 | 9 | 39 | | | 2.62 | 8.0 |
| | | FDAES | 1.97 | 139 | 9 | 279 | 2.13 | −171 | | |
| | measured[c] | GS | | | | | (≤0.8)[d] | (220) | | |
| **3** | B3LYP | GS | −0.69 | 519 | −39 | 133 | | | 2.57 | −48 |
| | | FDAES | −8.21 | 238 | 220 | −4900 | −7.52 | −281 | | |
| | | Relaxed $S_1$[e] | −5.85 | 295 | 566 | – | | | 1.43 | |
| | B3P86 | GS | −0.76 | 529 | −42 | 138 | | | 2.63 | −50 |
| | | FDAES | −8.09 | 205 | 221 | −4700 | −7.33 | −324 | | |
| | M06 | GS | −0.79 | 542 | −44 | 1425 | | | 2.70 | −52 |
| | | FDAES | −7.69 | 320 | 233 | ~−1500 | −6.90 | −222 | | |
| | CAM-B3LYP | GS | −0.23 | 405 | −11 | 5000 | | | 2.29 | −16 |
| | | FDAES | −7.59 | 834 | 136 | – | −7.36 | 429 | | |
| | RASPT2(18,18) | | | | | | −6.44 | | 2.03 | −26 |
| | literature[f] | GS | | | | | −6.16 | | 2.54 | −33 |
| | measured[g] | GS | | | | | (5.4)[d] | (230) | 2.10 | 28 |
| **4** | B3LYP | GS | −2.35 | 1035 | −116 | 6800 | | | 3.83/4.21 | −186/−214 |
| | | FDAES | −13.06 | 1158 | 917 | −21 000 | −10.71/−3.26 | 123 | | |
| | B3P86 | GS | −2.42 | 1057 | −126 | 7300 | | | 3.87 | −232 |
| | | FDAES | −12.94 | 1025 | 912 | −23 720 | −12.52 | −32 | | |
| | M06 | GS | −2.45 | 1063 | −127 | 7240 | | | 3.94 | −195 |
| | | FDAES | −12.50 | 1265 | 809 | −28 900 | −10.05 | 198 | | |
| | CAM-B3LYP | GS | −1.69 | 766 | −19 | 1354 | | | 4.79/1.80 | −70/−76 |
| | | FDAES | −7.74 | 3200 | −51 | – | −6.05/−5.42 | 2434 | | |
| | literature[f] | GS | | | | | −9.54 | | 3.58/3.78 | −130/−82 |
| | measured[g] | GS | | | | | (8.8)[d] | | 3.10/2.70 | 126 |

[a] All data calculated in $H_2O$ (**2**) or MeCN (**3** and **4**); **3** and **4** optimised in vacuum, **2** optimised in $H_2O$. [b] 2SA = two-state approximation; 3SA = three-state approximation. $\beta$ calculated from $6\Sigma_{i=1}^{n}\Delta_{0i}\mu_z(\mu_{0i})^2/(E_{0i})^2$ where $\mu_{0i}$ is the transition dipole-moment and $E_{0i}$ is the transition energy from the GS to the FDAES (i = 1) or SDAES (i = 2); $n = 1$ (2) for $\beta_{2SA}$ ($\beta_{3SA}$); an additional term for 3SA containing $\mu_{12}$ was neglected because this property computed in the gas-phase is almost zero. The value for **4** is the total obtained by applying the 2SA to the two low-energy absorption bands separately (the lowest energy band with MLCT character involves the FDAES, whereas the other band has intraligand charge-transfer character and involves the SDAES).[20] [c] Data for [**2**][$BF_4$]$_3$ taken from ref. [18]; numbers in brackets indicate properties measured in (or derived from data measured in) PrCN glasses. [d] Only the magnitude was determined. [e] Optimised structure in $S_1$ state. [f] Data taken from ref. [24]. [g] Data for [**3/4**][$PF_6$]$_3$ taken from ref. [20] and [21].

of the TD-DFT excited-state dipole-moments, and are thus *static* (zero-frequency) values.

Most of the FDAES properties were computed for the optimised GS geometries.[32] Nevertheless, in order to assess the possible effects of excited-state structural relaxation on the properties, an excited-state optimisation of **3** in the gas-phase was carried out, and properties were calculated also for the resulting geometry (see the Computational Methods for details).

The CAM-B3LYP results are again clearly very different from those obtained with the other functionals. Previously measured $\Delta_{01}\mu_z$ and $\Delta_{01}\alpha_{zz}$ values were obtained by Stark spectroscopy at 77 K in glassy PrCN solution, and are thus not directly comparable to computed values in liquid MeCN. Nevertheless, the latter are of the right order of magnitude when using B3LYP, B3P86 or M06. Interestingly, $\alpha_{zz}$ is predicted to be smaller for the FDAES than for the GS for **2** and **3**, but the reverse is apparent for **4** when using B3LYP or M06.[33] The calculations with B3LYP, B3P86 or M06 all predict the observed increases in $\Delta_{01}\mu_z$ on moving along the series **2**→**4**, and the Stark-based value of 8.8 au for **4**[21] is closest to that obtained when using M06.

The GS first hyperpolarisability of complex **3** in the two-state approximation ($\beta_{2SA}$) from RASPT2(18,18) is very close to the value deduced from experimental HRS data (28 472 au).[19] The corresponding values from the DFT methods are considerably larger; the reason for this can be traced back primarily to a substantially larger transition dipole-moment predicted by the DFT methods, which is squared in the equation for $\beta_{2SA}$, and is approximately 1.2–1.3-times larger than the RASPT2 result. Also, the DFT calculations give slightly larger dipole-moment changes than does RASPT2.

We find that the presence of diffuse functions in the basis set used to describe the first and second row atoms, which is generally of great importance for the NLO properties of the GS, has little influence on the NLO properties of the FDAES. The same can be said, to a lesser degree, of polarised functions, which generally are considered to be important for reliable descriptions of excited states. These obser-

vations appear quite unusual. On the other hand, the basis set LAN2TZ(f) for Ru is about the minimum necessary for a reliable description of both the GS and FDAES properties. This last factor explains the main differences between our data and those obtained by Inerbaev et al. and by Zhang and Champagne, who used the smaller basis set LAN2DZ.[23,24]

When considering the $\beta$ responses calculated by using B3LYP, B3P86 or M06, these increase substantially (as expected) on increasing the π-conjugation path-length along the series **2**→**4**, for both the GS and FDAES species (Table 2). Also, substantial enhancements are found for the FDAES with respect to the GS in each complex, with changes of similar magnitude predicted when using the three different functionals. However, the $\beta$ values calculated by using CAM-B3LYP show less consistent trends. Hence, although the GS $Ru^{II}$-containing chromophores possess large NLO responses, the activity is even larger for the MLCT excited states that formally contain $Ru^{III}$ coordinated to a reduced pyridyl ligand radical. The predicted excited-state enhancement of $\beta$ becomes more significant as the π-conjugated system extends, being about threefold for **2**, approximately fivefold for **3** and about sevenfold for **4**. For **3**, geometry relaxation within the FDAES (the $S_1$ state) leads to further considerable enhancement of $\beta$, whereas $\alpha$ increases slightly.

The cubic NLO properties, denoted by the second hyperpolarisability $\gamma$, are generally more difficult to compute reliably with our method, and thus should be considered as more approximate. Even so, they are also generally increased in the FDAES (Table 2). However, unlike for $\beta$, the results vary between the functionals B3LYP, B3P86 and M06. Using B3LYP or B3P86 yields enhancements of $\gamma$ in each case, but these are much larger for **3** (ca. 34–37-fold) when compared with **2** or **4** (ca. two- to sixfold). In contrast, the calculations with M06 predict an excitation-induced increase in $\gamma$ for **4** only (ca. fourfold), whereas no change is evident for **3** and a *decrease* is found for **2**. Unfortunately, no experimentally measured $\gamma$ values are available for **2**–**4** to allow comparisons with theory, because these complexes are of interest primarily for their quadratic NLO properties. The general result that both $\beta$ and $\gamma$ are larger in the FDAES is consistent with previous studies involving other types of chromophore.[8–11]

## Conclusion

Compared with previous computational studies on the electronic excitation and GS quadratic NLO properties of $Ru^{II}$ ammine complexes, we have used a larger basis set (LANL2TZ(f) for Ru) in DFT calculations. Also, we have used different larger basis sets for various high-level ab initio methods. TD-DFT calculations with the hybrid functionals B3LYP, B3P86 or M06 and a MeCN PCM yield very good agreement with the experimental spectrum for excitations to the FDAES of **3**. The same methods give a lower degree of matching with the experimental data for the shorter or longer complexes, underestimating $\lambda_{max}$ for **2**, but overestimating it for **4**. In each case, the calculations confirm the expected MLCT character of the FDAES. A model developed by Bahers et al. affords electron-transfer distances that agree well with those determined via Stark spectroscopic measurements on $[\mathbf{3}][PF_6]_3$ and $[\mathbf{4}][PF_6]_3$ previously. Notably, the results obtained for **3** by using B3LYP, B3P86 or M06 are very similar to those from RASPT2 with a very large basis set and large active space, both in solution and the gas-phase. Surprisingly, $\lambda_{max}$ values predicted by the long-range corrected functionals CAM-B3LYP, LC-ωPBE and wB97XB are less accurate than those obtained with B3LYP, B3P86 or M06 for all three complexes. Gas-phase results from the fully ab initio RI-CC2 method differ substantially from those derived from DFT and RASPT2, possibly due to the relatively high multi-configurational character of the GS.

Considering both the GS and FDAES, polarisabilities and hyperpolarisabilities were computed by finite-field derivatives of the TD-DFT excited-state dipole-moments, by using the functionals B3LYP, B3P86 or M06. The $\Delta_{01}\mu_z$ and $\Delta_{01}\alpha_{zz}$ values are of magnitude similar to those measured previously by Stark spectroscopy in the frozen solution state at 77 K. The GS $\beta_{2SA}$ value for **3** from RASPT2(18,18) is very close to that derived experimentally by HRS, whereas the corresponding DFT-based values are considerably larger, primarily due to substantially larger predicted $\mu_{01}$ values. Somewhat surprisingly, the presence of diffuse and polarised functions in the basis set used to describe the first and second row atoms has little influence on the NLO properties of the FDAES. As expected, the $\beta$ responses calculated by using B3LYP, B3P86 or M06 increase markedly as the π-conjugation extends along the series **2**→**4**, for both the GS and FDAES species. Also, substantial enhancements are found for the FDAES with respect to the GS in each complex, with the three different functionals predicting changes of similar magnitude. The excited-state enhancement of $\beta$ increases as the π-conjugation extends, from approximately threefold for **2** to about sevenfold for **4**. Although more approximate and of less interest for the complexes studied, the computed $\gamma$ values also generally increase in the FDAES, but the results vary between the functionals B3LYP, B3P86 and M06.

In summary, state-of-the-art theoretical methods show that MLCT excitation of $Ru^{II}$ ammine chromophores leads to large increases in molecular NLO responses. Therefore, such complexes hold promise not only as redox-switchable species, but also for ultrafast photoswitching of bulk NLO effects in appropriate organised media, such as LB thin films.

## Computational Methods

The molecules **2** and **3** were optimised with the 6-31G** basis set for CHN and the LANL2TZ(f) ECP/basis set for Ru at the DFT level with

  

the B3LYP functional. For **4**, the 6-31G basis was used for H. Molecule **2** was optimised in the gas-phase and in aqueous solution, by using the PCM, and the respective structures used for corresponding phase computations; for **3** and **4**, gas-phase optimised structures were used for all calculations except for the RASPT2 computations (see below).

Excited-state optimisation of **3** in the gas-phase was carried out with three different basis sets for the atoms H, C, N, O: 6-31G**, 6-31+G** and 6-31++G**, while LANL2TZ(f) was applied to Ru throughout. In order to be comparable with the other calculations, the properties were computed with the 6-31G** basis set and the PCM/MeCN model. The results can be grouped into two different sets according to the basis sets underlying the excited-state optimisation. With the 6-31+G**-optimised structure, a small Stokes shift, $\Delta_{St}$, of 0.28 eV was obtained, with a large oscillator strength for the transition to $S_0$ ($f_{os}=0.43$). This is approximately in line with the results reported by Zhang and Champagne,[24] ($\Delta_{St}=0.25$ eV, $f_{os}=0.31$), who apparently also used this basis set for the excited-state optimisation, although with LANL2DZ for Ru, the B3P86 functional and the PCM/MeCN model already applied during the optimisation. However, contrary to their result of the relaxed state being $S_1$, we find it to be $S_3$, which is also the Franck–Condon state. Usually, such a highly excited state would relax into $S_1$ by internal conversion before geometry relaxation is completed. For the 6-31G** and 6-31++G**-optimised structures, on the other hand, the relaxed state becomes $S_1$, showing large $\Delta_{St}$ values (1.2 and 1.1 eV for the 6-31G** and 6-31++G** optimised structure, respectively) and small $f_{os}$ values for dipolar transitions into $S_0$ (0.05 for both structures), which is in reasonable agreement with the absence of luminescence observed experimentally. Consequently, we used the 6-31G**-optimised structure to compute the excited-state properties. However, it should be noted that the optimisations of the second group were not fully successful in terms of the required criteria applied in Gaussian 09, even after about one hundred cycles. The best structures were finally used, where three of the four criteria were fulfilled.

TD-DFT with several functionals was employed to compute transition moments and excited-state dipole moments, which in turn were used for finite-field numerical differentiations to obtain the hyperpolarisabilities in the FDAES. The dipole moments of the charged species are reported with respect to the centre of nuclear charge. The GS properties were calculated analytically or by finite-field differences from GS dipole moments. Only the dominant long-axis component (oriented in $z$-direction) was computed in all cases. Most of the PCM excited-state calculations were performed by using the state-specific description for the non-equilibrium solvation during a vertical excitation,[34] although the differences when compared with the linear response non-equilibrium approximation[35] were generally negligible. The transition energies were measured from the electronic GS minimum, and no vibrational averages were taken into account. It should be noted that the comparison of computed vertical excitation energies with the experimental absorption maxima is only an approximation. A more accurate method would take the Franck–Condon factors (overlap between the vibrational wavefunctions of ground and excited electronic states) into account also. However, such an approach is computationally much more expensive,[36] and has thus not been used here. The useable field strengths for the finite-field numerical differentiations had to be adapted for each molecule and functional individually: the lowest useful field strengths depended on the magnitude of the properties, while the high-field limit was set by field-induced state mixing and switching. Gaussian 09[37] was used for these calculations.

The RI-CC2 calculations were carried out with Turbomole.[38] For the RASPT2 calculations on complex **3**, its structure was first optimised at the PBE0/TZVP/MWB-28(Ru) level in $C_s$ symmetry with Turbomole. Although this structure is not a minimum, the symmetry was required to make the multi-configurational calculations manageable. Tests with this structure at the DFT level showed that the influence of the non-minimum structure on the properties of interest is minimal. State-averaged RASPT2 calculations with extended ANO-rcc basis sets, ([8s7p6d3f2g1h] (Ru), [4s3p2d1f] (C,N), [3s2p1d] (H)) were then performed on this structure with Molcas.[39] Extensive tests were performed to find the optimal active space. These led finally to the following partition: the RAS2 space contains eight orbitals, five of Ru 4d parentage, two of their σ bonding counterparts and the π-orbital involved in the FDAES. RAS1 contains four π-orbitals and RAS3 three π* and three Ru 5d orbitals. Single and double excitations were allowed out of RAS1 and into RAS3, while all kinds of excitations were allowed in the RAS2 space.

For the three-state approximation of the first hyperpolarisability of **4** shown in Table 2, the excited-state dipole-moment between the FDAES and the second dipole-allowed excited state was computed with the Dalton2011 package,[40] in the gas phase. As the resulting value was very low, the corresponding term in the sum-over-states expression was neglected. Finally, the difference electronic density calculations were performed by using the CT program.[41]

## Acknowledgements

We thank the EPSRC (grants EP/G02099 and EP/J018635) for support of this work. A.A., H.R. and M.G.P. acknowledge funding provided by the European Commission for the FP7-REGPOT-2009-1 Project "ARCADE" (grant agreement no.: 245866), funding from the project "High Performance computing for South East Europe's Research Communities" (HP-SEE) and a grant in computing time provided by the "Partnership for Advanced Computing in Europe" (PRACE). K.P. and S.V. thank the Flemish Research Foundation (FWO) for research grants.

[1] a) J. Zyss, *Molecular Nonlinear Optics: Materials, Physics and Devices*, Academic Press, Boston, **1994**; b) Ch. Bosshard, K. Sutter, Ph. Prêtre, J. Hulliger, M. Flörsheimer, P. Kaatz, P. Günter, *Organic Nonlinear Optical Materials: Advances in Nonlinear Optics, Vol. 1.*, Gordon & Breach, Amsterdam, **1995**; c) *Nonlinear Optics of Organic Molecules and Polymers* (Eds.: H. S. Nalwa, S. Miyata), CRC, Boca Raton **1997**; d) S. R. Marder, *Chem. Commun.* **2006**, 131–134; e) *Nonlinear Optical Properties of Matter: From Molecules to Condensed Phases* (Eds.: M. G. Papadopoulos, J. Leszczynski, A. J. Sadlej), Springer, Dordrecht, **2006**.

[2] Recent reviews: a) H. Le Bozec, T. Renouard, *Eur. J. Inorg. Chem.* **2000**, 229–239; b) S. Barlow, S. R. Marder, *Chem. Commun.* **2000**, 1555–1562; c) P. G. Lacroix, *Eur. J. Inorg. Chem.* **2001**, 339–348; d) S. Di Bella, *Chem. Soc. Rev.* **2001**, *30*, 355–366; e) E. Goovaerts, W. E. Wenseleers, M. H. Garcia, G. H. Cross, in *Handbook of Advanced Electronic and Photonic Materials and Devices, Vol. 9* (Ed.: H. S. Nalwa), Academic Press, San Diego, **2001**, pp. 127–191; f) B. J. Coe, in *Comprehensive Coordination Chemistry II, Vol. 9* (Eds.: J. A. McCleverty, T. J. Meyer), Elsevier, Oxford, **2004**, pp. 621–687; g) O. Maury, H. Le Bozec, *Acc. Chem. Res.* **2005**, *38*, 691–704; h) E. Cariati, M. Pizzotti, D. Roberto, F. Tessore, R. Ugo, *Coord. Chem. Rev.* **2006**, *250*, 1210–1233; i) B. J. Coe, *Acc. Chem. Res.* **2006**, *39*, 383–393; j) M. E. Thompson, P. E. Djurovich, S. Barlow, S. Marder, in *Comprehensive Organometallic Chemistry III, Vol. 12* (Eds.: R. H. Crabtree, D. M. P. Mingos), Elsevier, Oxford, **2006**, pp. 101–194; k) C. Zhang, Y.-L. Song, X. Wang, *Coord. Chem. Rev.* **2007**, *251*, 111–141; l) J. P. Morrall, G. T. Dalton, M. G. Humphrey, M. Samoc, *Adv. Organomet. Chem.* **2007**, *55*, 61–136; m) C. Andraud, O. Maury, *Eur. J. Inorg. Chem.* **2009**, 4357–4371; n) S. Di Bella, C. Dragonetti, M. Pizzotti, D. Roberto, F. Tessore, R. Ugo, *Top. Organomet. Chem.* **2010**, *28*, 1–55; o) O. Maury, H. Le Bozec, in *Molecular Materials* (Eds.: D. W. Bruce, D. O'Hare, R. I. Walton), Wiley, Chichester, **2010**, pp. 1–59; p) B. J. Coe, *Coord. Chem. Rev.* **2013**, *257*, 1438–1458.

[3] a) B. J. Coe, *Chem. Eur. J.* **1999**, *5*, 2464–2471; b) I. Asselberghs, K. Clays, A. Persoons, M. D. Ward, J. A. McCleverty, *J. Mater. Chem.* **2004**, *14*, 2831–2839; c) K. A. Green, M. P. Cifuentes, M. Samoc, M. G. Humphrey, *Coord. Chem. Rev.* **2011**, *255*, 2530–2541.

[4] B. J. Coe, S. Houbrechts, I. Asselberghs, A. Persoons, *Angew. Chem.* **1999**, *111*, 377–380; *Angew. Chem. Int. Ed.* **1999**, *38*, 366–369.

[5] a) L. Boubekeur-Lecaque, B. J. Coe, K. Clays, S. Foerier, T. Verbiest, I. Asselberghs, *J. Am. Chem. Soc.* **2008**, *130*, 3286–3287; b) L. Boubekeur-Lecaque, B. J. Coe, J. A. Harris, M. Helliwell, I. Asselberghs, K. Clays, S. Foerier, T. Verbiest, *Inorg. Chem.* **2011**, *50*, 12886–12899.

[6] Selected examples: a) I. Asselberghs, K. Clays, A. Persoons, A. M. McDonagh, M. D. Ward, J. A. McCleverty, *Chem. Phys. Lett.* **2003**, *368*, 408–411; b) C. Sporer, I. Ratera, D. Ruiz-Molina, Y.-X. Zhao, J. Vidal-Gancedo, K. Wurst, P. Jaitner, K. Clays, A. Persoons, C. Rovira, J. Veciana, *Angew. Chem.* **2004**, *116*, 5378–5381; *Angew. Chem. Int. Ed.* **2004**, *43*, 5266–5268; c) M. P. Cifuentes, C. E. Powell, J. P. Morrall, A. M. McDonagh, N. T. Lucas, M. G. Humphrey, M. Samoc, S. Houbrechts, I. Asselberghs, K. Clays, A. Persoons, T. Isoshima, *J. Am. Chem. Soc.* **2006**, *128*, 10819–10832; d) M. Samoc, N. Gauthier, M. P. Cifuentes, F. Paul, C. Lapinte, M. G. Humphrey, *Angew. Chem.* **2006**, *118*, 7536–7539; *Angew. Chem. Int. Ed.* **2006**, *45*, 7376–7379; e) G. T. Dalton, M. P. Cifuentes, S. Petrie, R. Stranger, M. G. Humphrey, M. Samoc, *J. Am. Chem. Soc.* **2007**, *129*, 11882–11883; f) A. Wahab, M. Bhattacharya, S. Ghosh, A. G. Samuelson, P. K. Das, *J. Phys. Chem. B* **2008**, *112*, 2842–2847; g) W. Guan, G.-C. Yang, C.-G. Liu, P. Song, L. Fang, L. Yan, Z.-M. Su, *Inorg. Chem.* **2008**, *47*, 5245–5252; h) N. Gauthier, G. Argouarch, F. Paul, L. Toupet, A. Ladjarafi, K. Costuas, J.-F. Halet, M. Samoc, M. P. Cifuentes, T. C. Corkery, M. G. Humphrey, *Chem. Eur. J.* **2011**, *17*, 5561–5577.

[7] Selected examples: a) V. Aubert, V. Guerchais, E. Ishow, K. Hoang-Thi, I. Ledoux, K. Nakatani, H. Le Bozec, *Angew. Chem.* **2008**, *120*, 587–590; *Angew. Chem. Int. Ed.* **2008**, *47*, 577–580; b) Z.-H. Chen, S. Dong, C. Zhong, Z. Zhang, L.-H. Niu, Z.-Y. Li, F.-S. Zhang, *J. Photochem. Photobiol. A* **2009**, *206*, 213–219; c) K. A. Green, M. P. Cifuentes, T. C. Corkery, M. Samoc, M. G. Humphrey, *Angew. Chem.* **2009**, *121*, 8007–8010; *Angew. Chem. Int. Ed.* **2009**, *48*, 7867–7870; d) F. Mançois, J.-L. Pozzo, J.-F. Pan, F. Adamietz, V. Rodriguez, L. Ducasse, F. Castet, A. Plaquet, B. Champagne, *Chem. Eur. J.* **2009**, *15*, 2560–2571; e) A. Plaquet, B. Champagne, F. Castet, L. Ducasse, E. Bogdan, V. Rodriguez, J.-L. Pozzo, *New J. Chem.* **2009**, *33*, 1349–1356; f) E. Bogdan, L. Rougier, L. Ducasse, B. Champagne, F. Castet, *J. Phys. Chem. A* **2010**, *114*, 8474–8479; g) V. Guerchais, L. Ordronneau, H. Le Bozec, *Coord. Chem. Rev.* **2010**, *254*, 2533–2545; h) D. Marinotto, R. Castagna, S. Righetto, C. Dragonetti, A. Colombo, C. Bertarelli, M. Garbugli, G. Lanzani, *J. Phys. Chem. C* **2011**, *115*, 20425–20432; i) L. Ordronneau, H. Nitadori, I. Ledoux, A. Singh, J. A. G. Williams, M. Akita, V. Guerchais, H. Le Bozec, *Inorg. Chem.* **2012**, *51*, 5627–5636; j) P. Song, A.-H. Gao, P.-W. Zhou, T.-S. Chu, *J. Phys. Chem. A* **2012**, *116*, 5392–5397; k) H. Nitadori, L. Ordronneau, J. Boixel, D. Jacquemin, A. Boucekkine, A. Singh, M. Akita, I. Ledoux, V. Guerchais, H. Le Bozec, *Chem. Commun.* **2012**, *48*, 10395–10397.

[8] a) R. Sen, D. Majumdar, S. P. Bhattacharyya, S. N. Bhattacharyya, *Chem. Phys. Lett.* **1991**, *181*, 288–292; b) R. Sen, D. Majumdar, S. P. Bhattacharyya, S. N. Bhattacharyya, *J. Phys. Chem.* **1993**, *97*, 7491–7498.

[9] W. M. Faustino, D. V. Petrov, *Chem. Phys. Lett.* **2002**, *365*, 170–175.

[10] Selected examples: a) Q. L. Zhou, J. R. Heflin, K. Y. Wong, O. Zamani-Khamiri, A. F. Garito, *Phys. Rev. A* **1991**, *43*, 1673–1676; b) D. C. Rodenberger, J. R. Heflin, A. F. Garito, *Nature* **1992**, *359*, 309–311; c) J. R. Heflin, D. C. Rodenberger, R. F. Shi, M. Wu, N. Q. Wang, Y. M. Cai, A. F. Garito, *Phys. Rev. A* **1992**, *45*, R4233–R4236; d) D. C. Rodenberger, J. R. Heflin, A. F. Garito, *Phys. Rev. A* **1995**, *51*, 3234–3245; e) G. R. J. Williams, *J. Mol. Struct.* **1995**, *332*, 137–140; f) A. Oberlé, G. Jonusauskas, E. Abraham, C. Rullière, *Chem. Phys. Lett.* **1995**, *241*, 281–289; g) G. R. J. Williams, *Appl. Phys. B* **1996**, *63*, 47–50; h) C. Moreau, F. Serein-Spirau, J.-F. Létard, R. Lapouyade, G. Jonusauskas, C. Rullière, *J. Phys. Chem. B* **1998**, *102*, 1487–1497; i) W. Werncke, S. Hogiu, M. Pfeiffer, A. Lau, A. Kummrow, *J. Phys. Chem. A* **2000**, *104*, 4211–4217.

[11] a) A. Harada, T. Nagamura, *Proc. SPIE-Int. Soc. Opt. Eng.* **1998**, *3474*, 127–134; b) A. Harada, T. Nagamura, *Mol. Cryst. Liq. Cryst. Sect. B* **1999**, *22*, 169–172; c) T. Nagamura, T. Umeda, H. Sakaguchi, *Mol. Cryst. Liq. Cryst. Sci. Technol. A* **2001**, *370*, 119–122; d) D. V. Petrov, W. M. Faustino, *Opt. Commun.* **2002**, *203*, 145–150.

[12] a) H. Sakaguchi, T. Nagamura, T. Matsuo, *Jap. J. Appl. Phys. Part 2* **1991**, *30*, L377–L379; b) T. Nagamura, H. Sakaguchi, T. Matsuo, *Thin Solid Films* **1992**, *210/211*, 160–162; c) H. Sakaguchi, L. A. Gomez-Jahn, M. Prichard, T. L. Penner, D. G. Whitten, T. Nagamura, *J. Phys. Chem.* **1993**, *97*, 1474–1476; d) H. Sakaguchi, T. Nagamura, T. L. Penner, D. G. Whitten, *Thin Solid Films* **1994**, *244*, 947–950.

[13] a) J.-H. Si, Q.-G. Yang, Y.-G. Wang, P.-X. Ye, S.-B. Wang, J.-G. Qin, D.-Y. Liu, *Opt. Commun.* **1996**, *132*, 311–315; b) J. Zhao, Y.-G. Wang, J.-H. Si, P.-X. Ye, S.-J. Li, L.-J. Zhang, Z.-F. Wu, M.-J. Yang, *J. Nonlinear Opt. Phys. Mater.* **1997**, *6*, 109–117; c) W.-D. Cheng, D.-S. Wu, H. Zhang, J.-T. Chen, *J. Phys. Chem. B* **2001**, *105*, 11221–11226.

[14] B. J. Coe, J. A. Harris, B. S. Brunschwig, J. Garín, J. Orduna, S. J. Coles, M. B. Hursthouse, *J. Am. Chem. Soc.* **2004**, *126*, 10418–10427.

[15] Selected examples: a) C. M. Isborn, A. Leclercq, F. D. Vila, L. R. Dalton, J. L. Brédas, B. E. Eichinger, B. H. Robinson, *J. Phys. Chem. A* **2007**, *111*, 1319–1327; b) J. Lin, K.-C. Wu, M.-X. Zhang, *J. Comput. Chem.* **2009**, *30*, 2056–2063; c) K. Y. Suponitsky, Y. Liao, A. E. Masunov, *J. Phys. Chem. A* **2009**, *113*, 10994–11001; d) C. Cardoso, P. E. Abreu, B. F. Milne, F. Nogueira, *J. Phys. Chem. A* **2010**, *114*, 10676–10683.

[16] Selected examples: a) D. Jonsson, P. Norman, Y. Luo, H. Ågren, *J. Chem. Phys.* **1996**, *105*, 581–587; b) Y. Luo, P. Norman, D. Jonsson, H. Ågren, *Mol. Phys.* **1996**, *89*, 1409–1421; c) D. Jonsson, P. Norman, H. Ågren, Y. Luo, K. O. Sylvester-Hvid, K. V. Mikkelsen, *J. Chem. Phys.* **1998**, *109*, 6351–6357; d) F. C. Grozema, P. Th. van Duijnen, *J. Phys. Chem. A* **1998**, *102*, 7984–7989; e) F. C. Grozema, R. Telesca, H. T. Jonkman, L. D. A. Siebbeles, J. G. Snijders, *J. Chem. Phys.* **2001**, *115*, 10014–10021; f) F. C. Grozema, R. Telesca, J. G. Snijders, L. D. A. Siebbeles, *J. Chem. Phys.* **2003**, *118*, 9441–9446; g) R. Cammi, L. Frediani, B. Mennucci, K. Ruud, *J. Chem. Phys.* **2003**, *119*, 5818–5827; h) L. Ferrighi, L. Frediani, K. Ruud, *J. Chem. Phys.* **2010**, *132*, 024107–1–024107–12; i) K. Ruud, K. Gupta, T. K. Ghanty, S. K. Ghosh, *Phys. Chem. Chem. Phys.* **2010**, *12*, 2929–2934; j) B. Mennucci, R. Cammi, L. Frediani, in *Computational Aspects of Electric Polarizability Calculations: Atoms, Molecules and Clusters* (Ed.: G. Maroulis), IOS, **2004**, pp. 147–163.

[17] Selected examples: a) C. Creutz, H. Taube, *J. Am. Chem. Soc.* **1973**, *95*, 1086–1094; b) R. H. Magnuson, H. Taube, *J. Am. Chem. Soc.* **1975**, *97*, 5129–5136; c) J. F. Wishart, A. Bino, H. Taube, *Inorg. Chem.* **1986**, *25*, 3318–3321; d) J. R. Winkler, T. L. Netzel, C. Creutz, N. Sutin, *J. Am. Chem. Soc.* **1987**, *109*, 2381–2392; e) C. Creutz, M. H. Chou, *Inorg. Chem.* **1987**, *26*, 2995–3000.

[18] Y.-g. K. Shin, B. S. Brunschwig, C. Creutz, N. Sutin, *J. Phys. Chem.* **1996**, *100*, 8157–8169.

[19] B. J. Coe, J. A. Harris, L. J. Harrington, J. C. Jeffery, L. H. Rees, S. Houbrechts, A. Persoons, *Inorg. Chem.* **1998**, *37*, 3391–3399.

[20] B. J. Coe, J. A. Harris, B. S. Brunschwig, *J. Phys. Chem. A* **2002**, *106*, 897–905.

[21] B. J. Coe, L. A. Jones, J. A. Harris, B. S. Brunschwig, I. Asselberghs, K. Clays, A. Persoons, J. Garín, J. Orduna, *J. Am. Chem. Soc.* **2004**, *126*, 3880–3891.

[22] a) A. Willetts, J. E. Rice, D. M. Burland, D. P. Shelton, *J. Chem. Phys.* **1992**, *97*, 7590–7599; b) H. Reis, *J. Chem. Phys.* **2006**, *125*, 014506–1–014506–9.

[23] T. M. Inerbaev, R. V. Belosludov, H. Mizuseki, M. Takahashi, Y. Kawazoe, *J. Chem. Theory Comput.* **2006**, *2*, 1325–1334.

[24] Y. Zhang, B. Champagne, *J. Phys. Chem. C* **2013**, *117*, 1833–1848.

[25] a) T. Le Bahers, C. Adamo, I. Ciofini, *J. Chem. Theory Comput.* **2011**, *7*, 2498–2506; b) D. Jacquemin, T. Le Bahers, C. Adamo, I. Ciofini, *Phys. Chem. Chem. Phys.* **2012**, *14*, 5383–5388; c) I. Ciofini, T. Le Bahers, C. Adamo, F. Odobel, D. Jacquemin, *J. Phys. Chem. C* **2012**, *116*, 11946–11955.

[26] T. Yanai, D. P. Tew, N. C. Handy, *Chem. Phys. Lett.* **2004**, *393*, 51–57.

  

[27] O. A. Vydrov, G. E. Scuseria, *J. Chem. Phys.* **2006**, *125*, 234109–1–234109–09.
[28] J.-D. Chai, M. Head-Gordon, *Phys. Chem. Chem. Phys.* **2008**, *10*, 6615–6620.
[29] a) M. G. Fraser, A. G. Blackman, G. I. S. Irwin, C. P. Easton, K. C. Gordon, *Inorg. Chem.* **2010**, *49*, 5180–5189; b) J. Guthmuller, L. González, *Phys. Chem. Chem. Phys.* **2010**, *12*, 14812–14821; c) D. Escudero, L. González, *J. Chem. Theory Comput.* **2012**, *8*, 203–213.
[30] a) O. Christiansen, H. Koch, P. Jørgensen, *Chem. Phys. Lett.* **1995**, *243*, 409–418; b) C. Hättig, F. Weigend, *J. Chem. Phys.* **2000**, *113*, 5154–5161; c) C. Hättig, A. Köhn, *J. Chem. Phys.* **2002**, *117*, 6939–6951.
[31] C. J. Cramer, D. G. Truhlar, *Phys. Chem. Chem. Phys.* **2009**, *11*, 10757–10816.
[32] The rationale for using the GS instead of the relaxed FDAES geometry is that the MLCT excited-state lifetimes ($\tau$) of complexes like **2**–**4** are very short; they give no detectable luminescence, and $\tau$ values of less than 30 ps have been determined for **2** and $[Ru^{II}(NH_3)_5(4,4'\text{-bpyH})]^{2+}$ (the protonated analogue of **3**) at room temperature in water; see ref. [17d]. Thus, it is not clear if a relaxed structure will be reached at all during the excited-state lifetime. In addition, a hypothetical pump-probe experiment could involve a time delay between the two pulses of a few fs, probing the excited molecules very soon after Franck–Condon excitation.
[33] The reductions of $\alpha_{zz}$ on excitation for **2** and **3** may be due to the comparatively large contribution of the term $-4\mu_{01z}\mu_{10z}/(E_1-E_0)$ in the SOS expression for $\Delta\alpha_{zz}$; see ref. [18]. This term contributes −284 au for **2** and −340 au for **3**, computed with the B3LYP/PCM results, and is thus of the same order of magnitude as the full finite-field values given in Table 2. However, these predictions are not corroborated experimentally. Although variation in physical conditions precludes direct experiment/theory comparisons, it is possible that the predicted decreases in $\alpha_{zz}$ are an artefact of the DFT method employed. Comparisons with high-level multi-configurational ab initio values may shed more light on this problem, and such investigations are in progress.
[34] R. Improta, V. Barone, G. Scalmani, M. J. Frisch, *J. Chem. Phys.* **2006**, *125*, 054103–1–054103–9.
[35] R. Improta, G. Scalmani, M. J. Frisch, V. Barone, *J. Chem. Phys.* **2007**, *127*, 074504–1–074504–9; c) M. Cossi, V. Barone, *J. Chem. Phys.* **2001**, *115*, 4708–4717.
[36] R. Improta, V. Barone, F. Santoro, *Angew. Chem.* **2007**, *119*, 409–412; *Angew. Chem. Int. Ed.* **2007**, *46*, 405–408.
[37] Gaussian 03 (Revision C.01), M. J. Frisch, G. W. Trucks, H. B. Schlegel, G. E. Scuseria, M. A. Robb, J. R. Cheeseman, J. A. Montgomery, Jr., T. Vreven, K. N. Kudin, J. C. Burant, J. M. Millam, S. S. Iyengar, J. Tomasi, V. Barone, B. Mennucci, M. Cossi, G. Scalmani, N. Rega, G. A. Petersson, H. Nakatsuji, M. Hada, M. Ehara, K. Toyota, R. Fukuda, J. Hasegawa, M. Ishida, T. Nakajima, Y. Honda, O. Kitao, H. Nakai, M. Klene, X. Li, J. E. Knox, H. P. Hratchian, J. B. Cross, V. Bakken, C. Adamo, J. Jaramillo, R. Gomperts, R. E. Stratmann, O. Yazyev, A. J. Austin, R. Cammi, C. Pomelli, J. W. Ochterski, P. Y. Ayala, K. Morokuma, G. A. Voth, P. Salvador, J. J. Dannenberg, V. G. Zakrzewski, S. Dapprich, A. D. Daniels, M. C. Strain, O. Farkas, D. K. Malick, A. D. Rabuck, K. Raghavachari, J. B. Foresman, J. V. Ortiz, Q. Cui, A. G. Baboul, S. Clifford, J. Cioslowski, B. B. Stefanov, G. Liu, A. Liashenko, P. Piskorz, I. Komaromi, R. L. Martin, D. J. Fox, T. Keith, M. A. Al-Laham, C. Y. Peng, A. Nanayakkara, M. Challacombe, P. M. W. Gill, B. Johnson, W. Chen, M. W. Wong, C. Gonzalez, J. A. Pople, Gaussian, Inc., Wallingford CT, **2004**..
[38] Turbomole V6.4, **2012**, a development of University of Karlsruhe and Forschungszentrum Karlsruhe GmbH, 1989–2007, Turbomole GmbH, since 2007; available from: http://www.turbomole.com.
[39] G. Karlström, R. Lindh, P.-Å. Malmqvist, B. O. Roos, U. Ryde, V. Veryazov, P.-O. Widmark, M. Cossi, B. Schimmelpfennig, P. Neogrady, L. Seijo, *Comput. Mater. Sci.* **2003**, *28*, 222–239; Molcas V6.4: http://www.molcas.org/.
[40] DALTON; a molecular electronic structure program, Release Dalton2011, **2011**: http://www.daltonprogram.org.
[41] See ref. [25c] and http://www.sciences.univ-nantes.fr/CEISAM/erc/marches.

Received: April 11, 2013
Published online: October 10, 2013